SYNOPTIC AND MESOSCALE FEATURES LEADING TO THE 10 MARCH 1992 CHARLOTTE, NORTH CAROLINA TORNADO: A LOW-TOP, WEAK-REFLECTIVITY, SEVERE WEATHER EVENT

Michael D. Vescio

National Weather Service Forecast Office*
Raleigh-Durham, North Carolina

Neil A. Stuart

National Weather Service Office**
Wilmington, North Carolina

Abstract

On 10 March 1992, a tornado of F2 intensity tracked through Charlotte, North Carolina, causing one fatality, numerous injuries, and significant damage. This study focuses on the synoptic and mesoscale features that created an environment favorable for tornado formation. An overview of the echo structure as viewed from the WSR-74C radar at Charlotte (CLT) is presented. The convection with this case was characterized by low-tops (less than 25,000 ft) and weak reflectivity (Digital Video Integrator and Processor [DVIP] level 3 or less), confirming that tornadoes are possible with relatively weak thunderstorms if there is strong low-level wind shear.

1. Introduction

On the evening of 10 March 1992, a strong tornado struck Charlotte, North Carolina (CLT) (for location, see Fig. 15). The tornado first touched down in the Steel Creek area on the southwest side of the city at approximately 2207 EST 10 March (0307 UTC 11 March). The tornado moved east-northeast, through the southern portion of Charlotte, where the most damage occurred, and then into neighboring Cabarrus and Stanly counties.

The discontinuous nature of the damage path suggests that the tornado was aloft for much of the time. However, when the vortex briefly touched down in Charlotte, significant damage occurred. One death and 27 injuries were attributed to the tornado. Three houses were destroyed, 27 suffered major damage and 25 sustained minor damage. In addition, many trees were uprooted in Cabarrus and Stanly counties.

Synoptic and mesoscale analyses are used to diagnose the severe storm potential for this case. In addition, soundings and hodographs are generated by the Skew T-Hodograph Analysis and Research Program (SHARP; Hart and Korotky 1991) to examine the stability and low-level wind shear profile.

2. Synoptic Analyses

a. Surface features

Figure 1 depicts the surface analysis at 0300 UTC 11 March, just prior to the tornado occurrence. The major features included a surface low centered in central Virginia, and a fast-moving cold front trailing through the western Carolinas and North Georgia. At this time, a large area of light rain and embedded thunderstorms was over coastal North Carolina, well ahead of the cold front. This area of precipitation was the remnants of thunderstorms that developed during the afternoon of the 10th in the piedmont of North Carolina. A few of these storms produced wind damage around 2100 UTC on the 10th.

b. Upper-air features

At 0000 UTC 11 March a low-level jet was present at the 850-mb level over central North Carolina (Fig. 2), where Greensboro (GSO) reported a 50 kt wind. Winds of 40 kt covered much of the eastern United States.

Mid-level drying was evident at 700 mb (Fig. 3), which according to Doswell (1982), is an important ingredient for severe convection. An analysis of dewpoint depressions showed considerable dry air (10°C depressions or greater) over most of North Carolina and northern South Carolina. It is difficult to determine the exact dewpoint depression near CLT, but based on the subjective analysis it is evident that at least some mid-level drying occurred in this area.

The 700-mb vertical velocity chart from the NWS/National Meteorological Center's Nested Grid Model (NGM) (Fig. 4) corresponded well with the areas of precipitation associated with this system. The area of showers and thunderstorms along the coast was located in a zone of 12 $\mu b\ s^{-1}$ upward vertical velocities. The negative vertical velocities over central North Carolina indicating subsidence, agreed well with the 500-mb wind field (Fig. 5) and vorticity pattern (Fig. 6). The translation of upward vertical velocity over Georgia at 0000 UTC, to the western Carolinas by 0300 UTC, further indicates a synoptic scale environment conducive to thunderstorm development.

At 300 mb (Fig. 7), a 130 kt jet streak extended across the Gulf coast eastward to western South Carolina at 0000 UTC. It appears that western North and South Carolina were in the left front quadrant of the jet streak, which is a region associated with upward vertical motion, and often severe weather.

3. Atmospheric Stability and Vertical Wind Shear

Figure 8 depicts the 0000 UTC 11 March sounding at Athens, Georgia (AHN). The sounding was marginally unstable, with a Lifted Index (LI) of −1. The Total Totals (TT) was only 42, largely due to the dry air at the 850-mb level. A dry layer (dewpoint depressions of approximately 10°C)

*Current affiliation: NWS National Severe Storms Forecast Center, Kansas City, Missouri.
**Current affiliation: NWS Weather Forecast Office, Wakefield, Virginia.

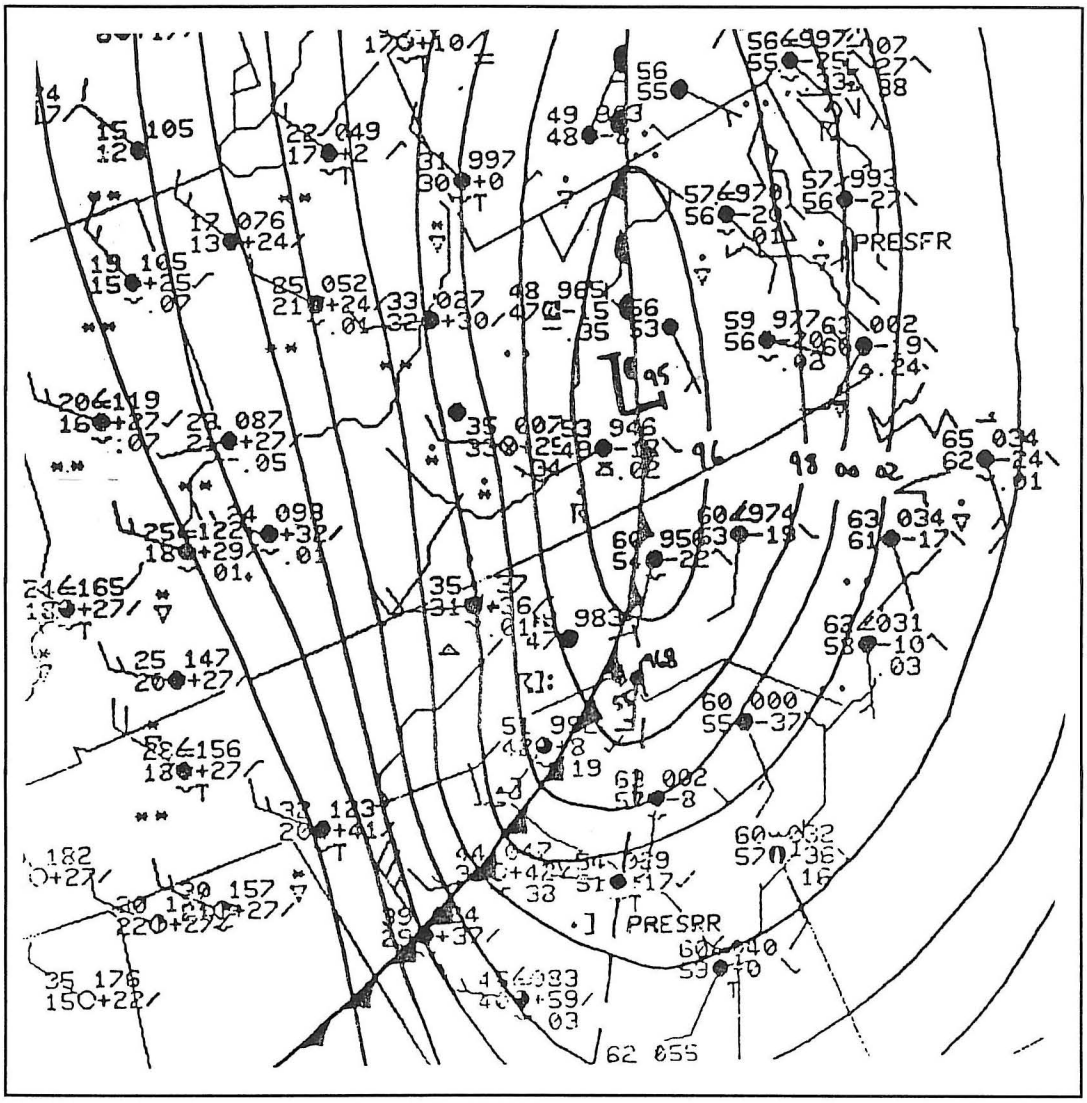

Fig. 1. Surface analysis for 0300 UTC 11 March.

extended from just below the 850-mb to the 700-mb level. As mentioned earlier, mid-level dry intrusions can enhance severe storm potential. This demonstrates the limitations of using indices based on mandatory levels for assessing stability. Rather than relying solely on convective indices, one should look at the entire sounding to determine the convective potential. Indeed, lapse rates were quite steep between 700 and 500 mb. SHARP computed a cooling rate of 9.1°C km^{-1} in this layer. A saturated air parcel rising through this layer would be highly buoyant. However, above this level, the stability increased, and parcels became negatively buoyant above 450 mb. Therefore, in this case, high storm tops and very high reflectivities should not have been expected.

Figure 9 depicts the 0000 UTC 11 March sounding at GSO. The sounding was relatively stable with a LI of +2 and a TT of 47. A mid-level dry intrusion was very prominent from about 800 mb to 500 mb. A capping inversion was present at approximately 800 mb. The cap strength was 2.8°C, which is above the critical value cited by Graziano and Carlson (1987). They indicate that caps greater than 2°C may inhibit or prevent convection. However, if a forcing mechanism can break or erode the cap, explosive convective development can occur, provided the air is unstable above the inversion. The lapse rate above the inversion at GSO was quite steep, nearly dry adiabatic, to about 620 mb.

A mechanism for cap erosion may have been the synoptic scale, upward vertical motion associated with the strong PVA and the advancing cold front. Synoptic scale ascent causes stable layers to become less stable (move toward a dry adiabatic lapse rate). This mechanism might explain why the cap at AHN (0.6°C) was much weaker than that at GSO at 0000 UTC.

Figures 10 and 11 are sounding hodographs at AHN and GSO for 0000 UTC 11 March. Substantial low-level clockwise turning is indicated on both hodographs, which favors right-moving supercells (Klemp 1987). The 0–3 km storm-relative (SR) helicity was 349 and 333 $m^2 s^{-2}$ (units henceforth dropped) at AHN and GSO, respectively. These values are valid for a storm moving almost due east at a speed of nearly 40 kt, which approximates the true storm motion based on a loop from the radar at CLT. Results from a study conducted

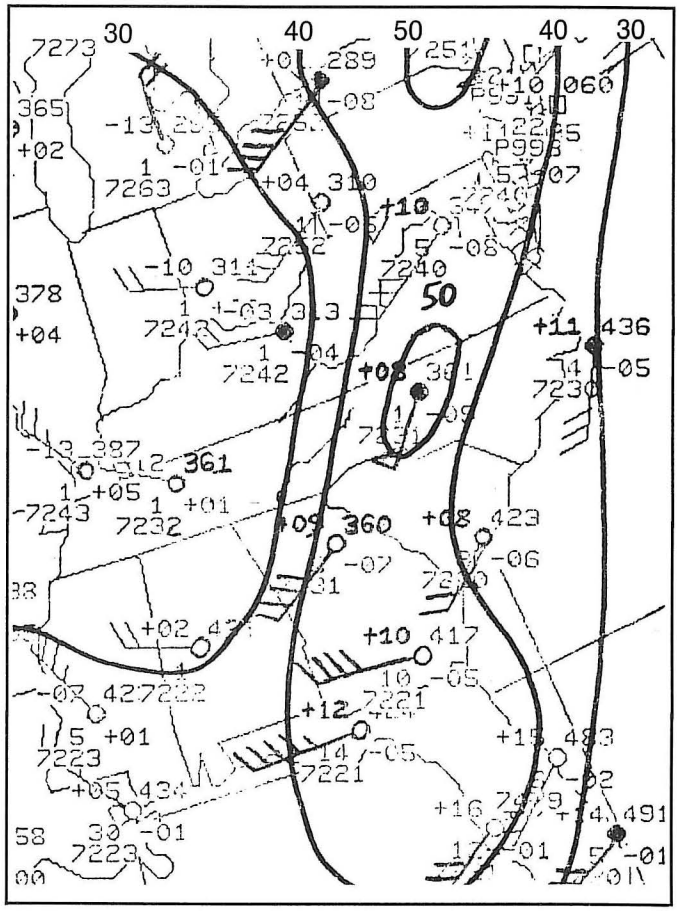

Fig. 2. 850-mb plot and isotach analysis (kt) for 0000 UTC 11 March.

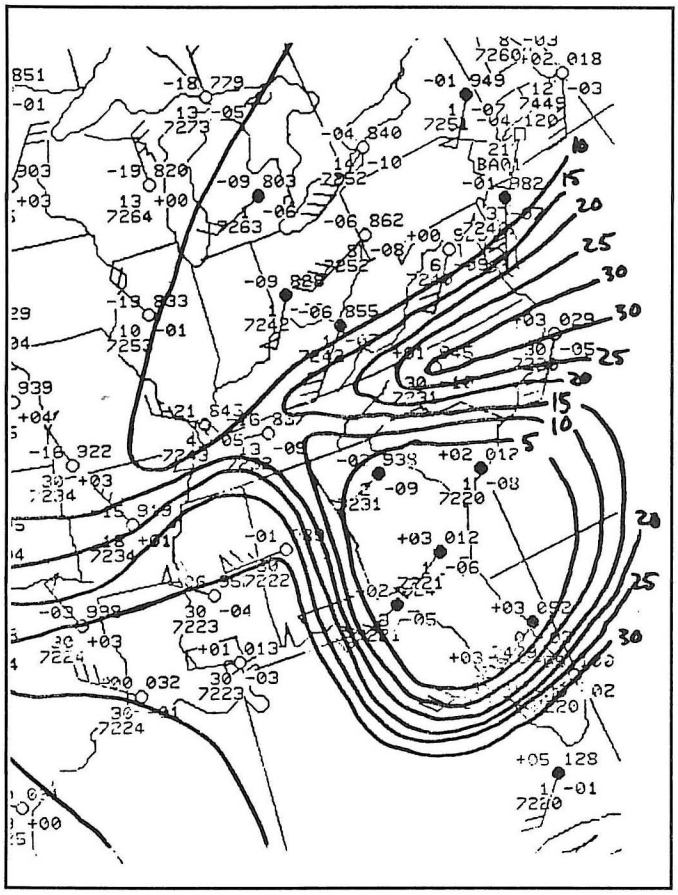

Fig. 3. 700-mb plot and dewpoint depression analysis (°C) for 0000 UTC 11 March.

by Davies-Jones et al. (1990) suggest that the minimum SR helicity threshold for mesocyclone formation is 150. In that study, helicity values for 28 tornadoes, of varying intensity, were calculated. Median helicity values for weak (F0–F1), strong (F2–F3) and violent (F4–F5) tornadoes were 278, 330, and 531 respectively. The observed ranges for each category were 150–299, 300–449, and >450. The helicity from both the AHN and GSO soundings indicated the potential for strong tornadoes, and in fact, the Charlotte tornado was rated F2.

Numerical simulations by Lazarus and Droegemeier (1990) revealed that the low-level (near the surface) storm inflow, in addition to SR helicity, may dictate whether a thunderstorm can acquire rotation. Their study indicated that regardless of the shear magnitude, rotating storms cannot develop if the storm inflow is less than 10 m s^{-1}, or approximately 20 kt. The mean low-level (0–3 km) inflow at AHN was 21 kt and the inflow at GSO was 28 kt, both above the suggested threshold.

In summary, despite marginal instability, the shear profile was very favorable for rotating thunderstorms. Once sufficient forcing initiated convection, the environment became suitable for mesocyclone formation.

4. Mesoscale Analyses

ADAP (AFOS Data Analysis Program; AFOS is the dissemination system used by the National Weather Service) output (Bothwell 1988) was used to examine the mesoscale features associated with this case. Many of the "classic" features that are expected with severe weather were not present. However, a few of the analyses gave some indication of severe weather potential.

Figures 12a–c are analyses of surface moisture flux convergence (AFOS graphic SMC) for 0100–0300 UTC. Moisture flux convergence (MFC) is very useful for assessing convective potential since it includes both the effects of low-level mass convergence, which leads to upward vertical motion, as well as moisture pooling, which destabilizes the atmosphere (Waldstreicher 1989). At 0100 UTC slightly positive values of MFC were in the threat area. At 0200 and 0300 UTC, a MFC maximum developed in northwest South Carolina. The tornadic storm occurred in an area downwind of the maximum (i.e., in the gradient area), which according to Waldstreicher (1989) is a preferred location for storm development.

The surface potential temperature (theta) advection charts (AFOS graphic STA) did not indicate a severe weather threat (Figures 13a–c). Cold advection occurred in the Charlotte area during the 2 hours prior to the tornado. Normally, one would expect warm advection in a severe weather environment since this destabilizes the atmosphere, and causes veering of the wind with height.

Finally, the surface streamline analysis (AFOS graphic SSW) (Figs. 14a–c) showed a zone of confluence across the Charlotte area that increased with time. Confluent flow generally produces upward vertical motion, which, as mentioned earlier, may be a mechanism for cap erosion.

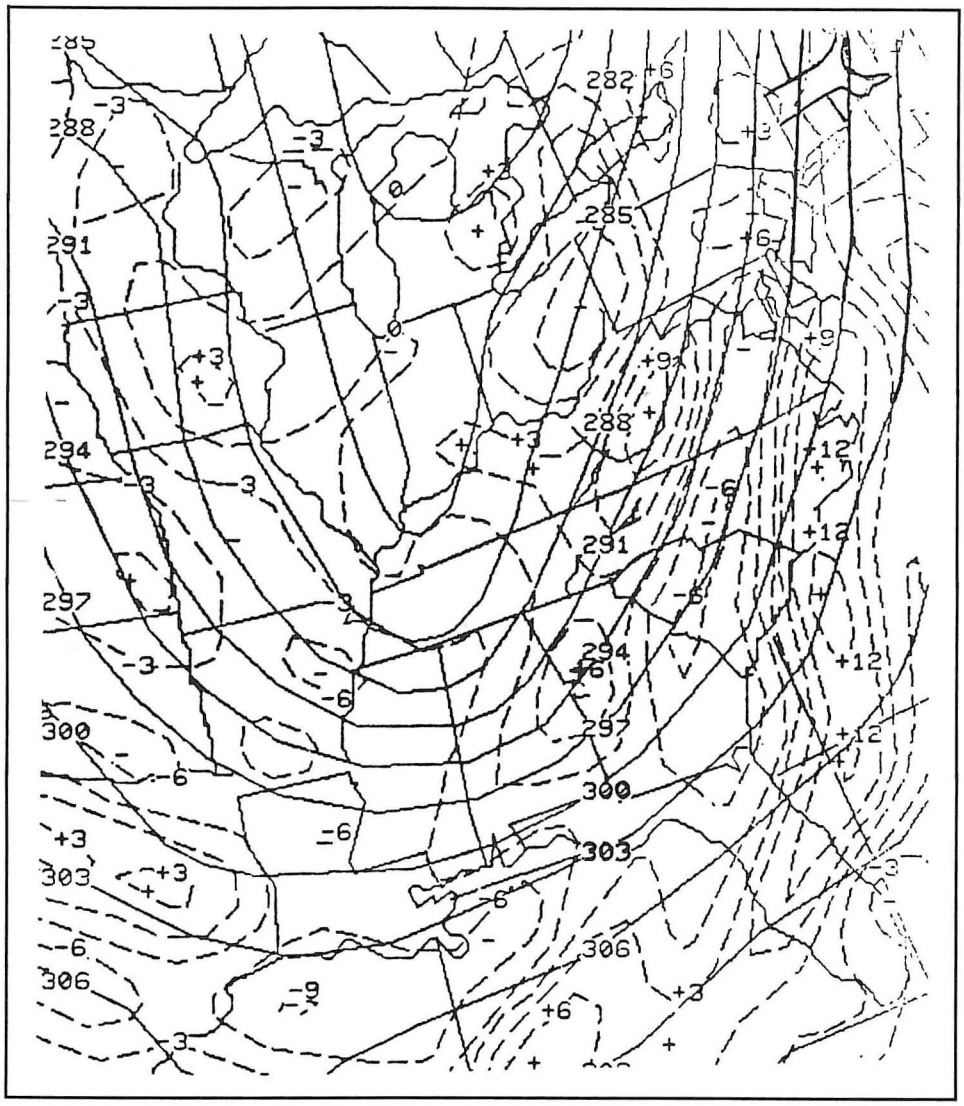

Fig. 4. 700-mb, 00-hour NGM vertical velocities ($\mu b\ s^{-1}$) for 0000 UTC 11 March.

5. Storm Evolution

The thunderstorm complex that moved into North Carolina and produced the Charlotte tornado initiated in western South Carolina shortly before 0000 UTC on the 11th. A line of storms formed in the upstate of South Carolina and evolved into a bow echo. Figure 15 depicts radar reflectivity (O.5° elevation) as observed from the radar at CLT at 0248 UTC, about 20 minutes prior to the tornado. A line of low-top (less than 25000 ft), low-reflectivity (DVIP 3 or less) thunderstorms extended from just west of CLT southward to west of Columbia (CAE). The line had a concave or bow shaped appearance across northern South Carolina. Another area of thunderstorms extended from near Hickory, North Carolina (HKY) to just west of Winston-Salem (INT). The thunderstorm located northeast of Greer (GSP) in northwest South Carolina produced wind damage and large hail along its path across upstate South Carolina into North Carolina, from west of CLT to near INT.

It is interesting how this mesoscale echo configuration resembled a synoptic scale wave cyclone, with a low pressure center over northwest South Carolina, a mesoscale cold front extending across South Carolina, and a warm front across western North Carolina. However, the mesoscale pressure field did not match this pattern. Subjective streamline analyses (not shown) did indicate significant cyclonic shear (slightly more than ADAP) over upstate South Carolina, suggesting that a mesolow (perhaps on a scale of 100 km, not to be confused with a mesocyclone), might have existed, but was too small to be fully resolved by the surface observing network. In addition, the surface geostrophic vorticity chart at 0300 UTC (Fig. 16) clearly shows a strong vorticity maximum just northwest of CLT; further evidence that a mesolow may have existed.

Figures 17 and 18 show the reflectivity pattern at 0301 and 0314 UTC. The tornado occurred at 0307 UTC. Unfortunately, the tornadic storm was embedded within the ground clutter of the CLT radar. Nonetheless, some inferences can

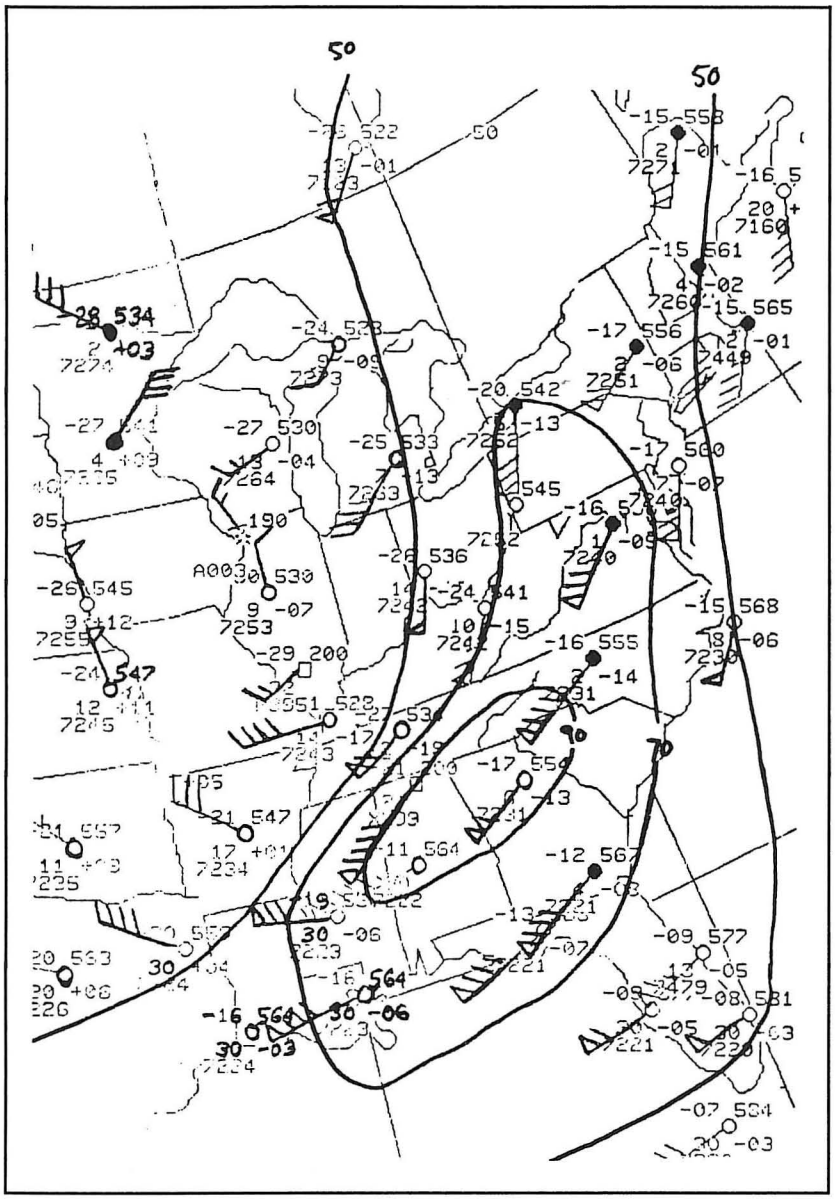

Fig. 5. 500-mb plot and isotach analysis (kt) for 0000 UTC 11 March.

be made from the reflectivity pattern. The tornado producing thunderstorm appeared to be on the northern end of the bow echo. Fujita (1978) states that bow echoes sometimes evolve into a comma shape, and that mesocyclone and tornado formation occasionally occurs in what he refers to as a "rotating comma head," on the northern end of a bow echo. It is impossible to prove, due to the ground clutter interference, but this seems like a plausible explanation.

6. Summary

On 10 March 1992, an F2 tornado struck Charlotte, North Carolina. One death, many injuries, and substantial property damage resulted from this tornado. The tornadic thunderstorm was on the northern edge of a well-defined bow echo, which Fujita (1978) indicates is a preferred location for mesocyclone formation. However, the ground clutter pattern surrounding the radar at CLT masked any conclusive evidence regarding the storm's structure. Many synoptic and mesoscale features combined to produce a favorable environment for severe convection and the resulting tornado, despite marginal instability.

The ADAP fields revealed some precursors to severe convection, including mass and moisture convergence. However, the theta fields indicated a cold advection pattern across the threat area. Perhaps a higher spatial resolution of surface data could have helped to resolve some of the small scale features that may have played a role in this case. This could be accomplished by the introduction of Automated Surface Observing System (ASOS) units in data sparse areas.

SHARP is a valuable resource for determining severe weather potential. Soundings and hodographs are easily modified as conditions change. The program also calculates low-level SR helicity and shear which have been determined

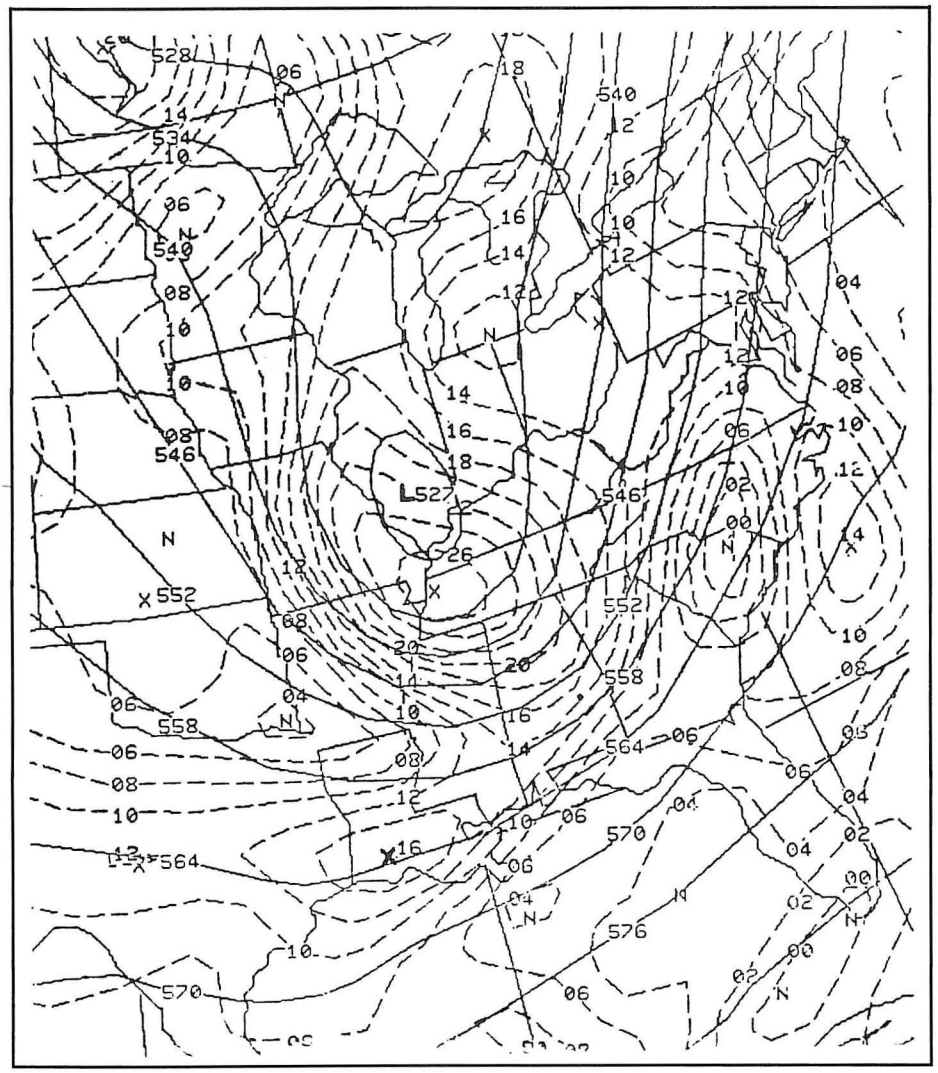

Fig. 6. 00-hour NGM height (dm) and vorticity ($\times 10^{-5}$ s^{-1}) analysis for 0000 UTC 11 March.

to be critical for the development of mesocyclones and tornadoes.

Finally, this case adds to the growing evidence that tornadic storms may exhibit considerably weaker radar returns than the "text book" examples of Great Plains supercells (particularly during the cold season; October–March). Forecasters must be aware that if the environment favors storm rotation, the storm structure is much more important than maximum reflectivities or storm tops. It would be useful to document more low-top, weak-reflectivity severe episodes to determine their relative frequency.

Acknowledgments

The authors thank Herb White, Mary McVicker and the Southeast Consortium on Severe Thunderstorms and Tornadoes for their assistance in generating mesoscale output and drafting of schematic radar displays.

Authors

Michael Vescio just transferred to the National Weather Service's (NWS) National Severe Storms Forecast Center in Kansas City, Missouri. He was previously a forecaster at the NWS Forecast Office in Raleigh-Durham, North Carolina, where he served since February 1992. He joined the NOAA/NWS in 1990 and began his career as a Meteorologist Intern at the NWS Forecast Office in Columbia, South Carolina. Mike received a M.S. degree in Atmospheric Science from Colorado State University in 1990. He earned a B.S. degree from The State University of New York (SUNY) at Oswego in 1988. Mike's primary interests are severe storms forecasting and research. He was the Program Chairman for the December 1993 NWA Annual Meeting in Raleigh.

Neil Stuart recently transferred to the NWS Weather Forecast Office in Wakefield, Virginia as a Journeyman Forecaster. He spent the past 3½ years as a Meteorologist Intern

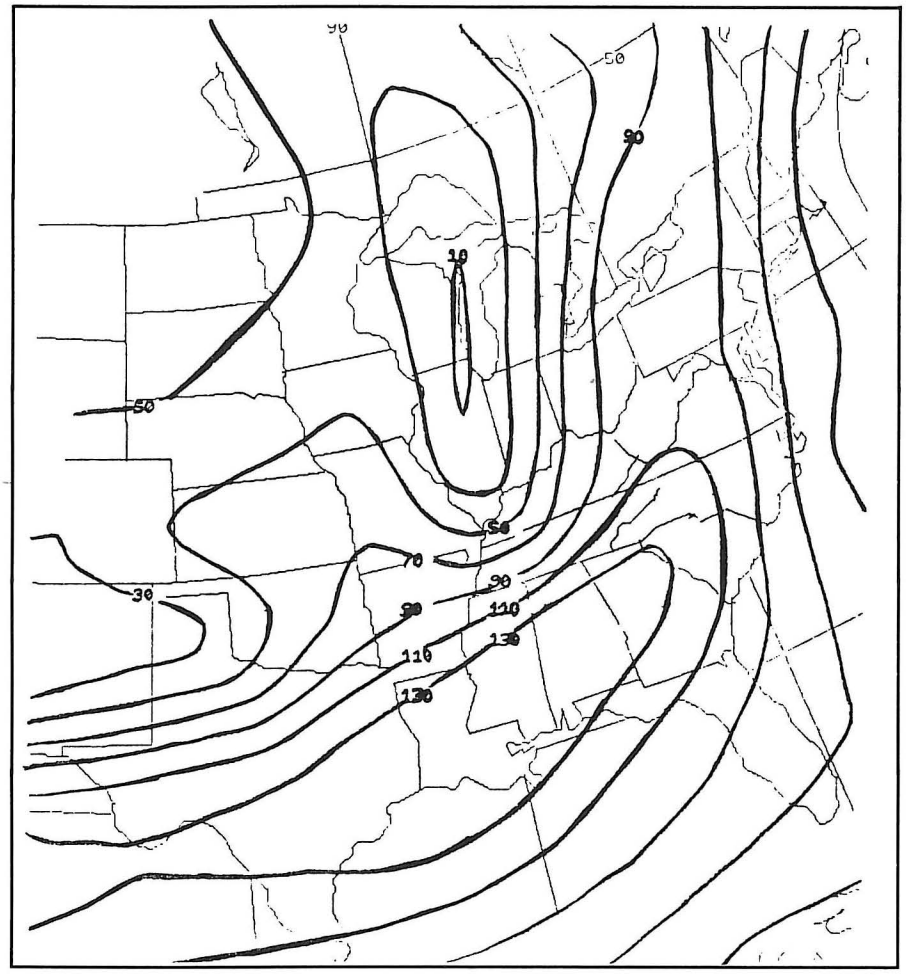

Fig. 7. 300-mb isotach analysis (kt) for 0000 UTC 11 March.

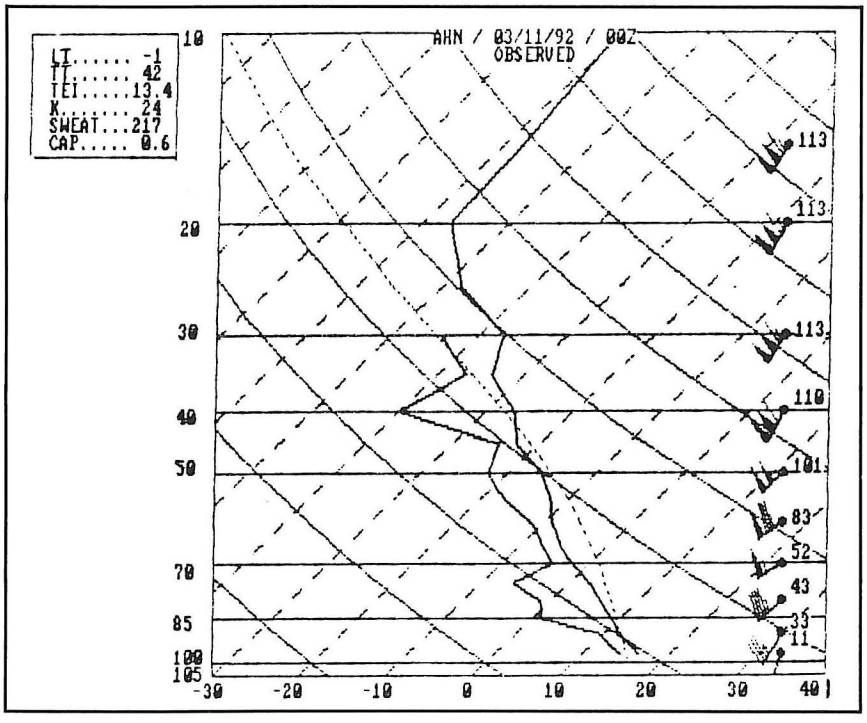

Fig. 8. Athens, GA (AHN) sounding for 0000 UTC 11 March.

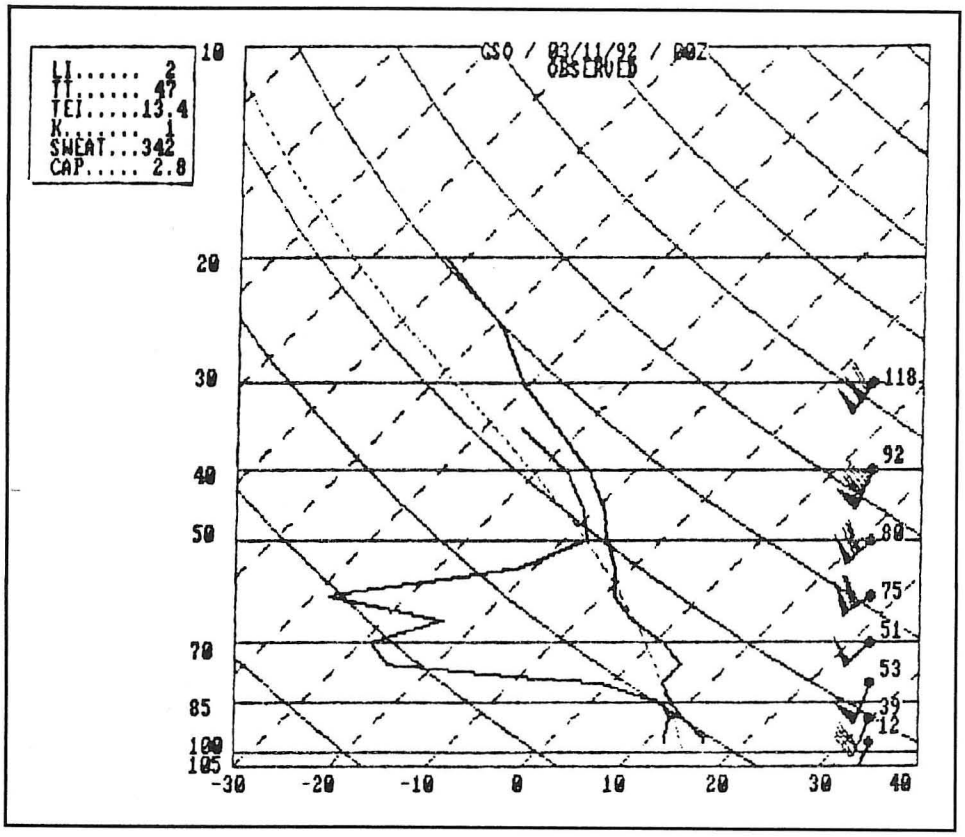

Fig. 9. Greensboro, NC (GSO) sounding for 0000 UTC 11 March.

at the National Weather Service Office in Wilmington, North Carolina. He received a B.S. degree in Meteorology from The State University of New York (SUNY) at Albany in 1990. His primary interests include severe weather forecasting and mesoscale analysis.

References

Bothwell P. D., 1988: Forecasting convection with the AFOS Data Analysis Program (ADAP—Version 2.0). *NOAA Tech. Memo. NWS SR-122*, U.S. Dept. of Commerce, 91 pp.

Davies-Jones R., D. W. Burgess, and M. P. Foster, 1990: Test of helicity as a tornado forecast parameter. *Preprints, 16th Conf. on Severe Local Storms*, Kananaskis Park, Canada, Amer. Meteor. Soc., 588–592.

Doswell, C. A. III, 1982: The operational meteorology of convective weather Volume I: Operational Mesoanalysis. *NOAA Tech. Memo. NWS NSSFC-5*, U.S. Dept. of Commerce, 164 pp.

Fujita, T. T., 1978: *Manual of Downburst Identification for Project Nimrod.* SMRP Res. Paper No 156, The University of Chicago, 104 pp.

Graziano, T. M., and T. M. Carlson, 1987: A statistical evaluation of lid strength on deep convection. *Wea. Forecasting*, 2, 127–139.

Hart J. A., and J. Korotky, 1991: *The SHARP workstation v1.50 user's manual.* National Weather Service, NOAA, U.S. Dept. of Commerce, 30 pp.

Klemp, J. B., 1987: Dynamics of tornadic thunderstorms. *Ann. Review of Fluid Mech.*, 19, 369–402.

Lazarus, S. M., and K. K. Droegemeier, 1990: The influence of helicity on the stability and morphology of numerically simulated storms. *Preprints, 16th Conf. on Severe Local Storms*, Kananaskis Park, Canada, Amer. Meteor. Soc., 269–274.

Waldstreicher, J. S. 1989: A guide to utilizing moisture flux convergence as a predictor of convection. *Nat. Wea. Dig.*, 14, 20–35.

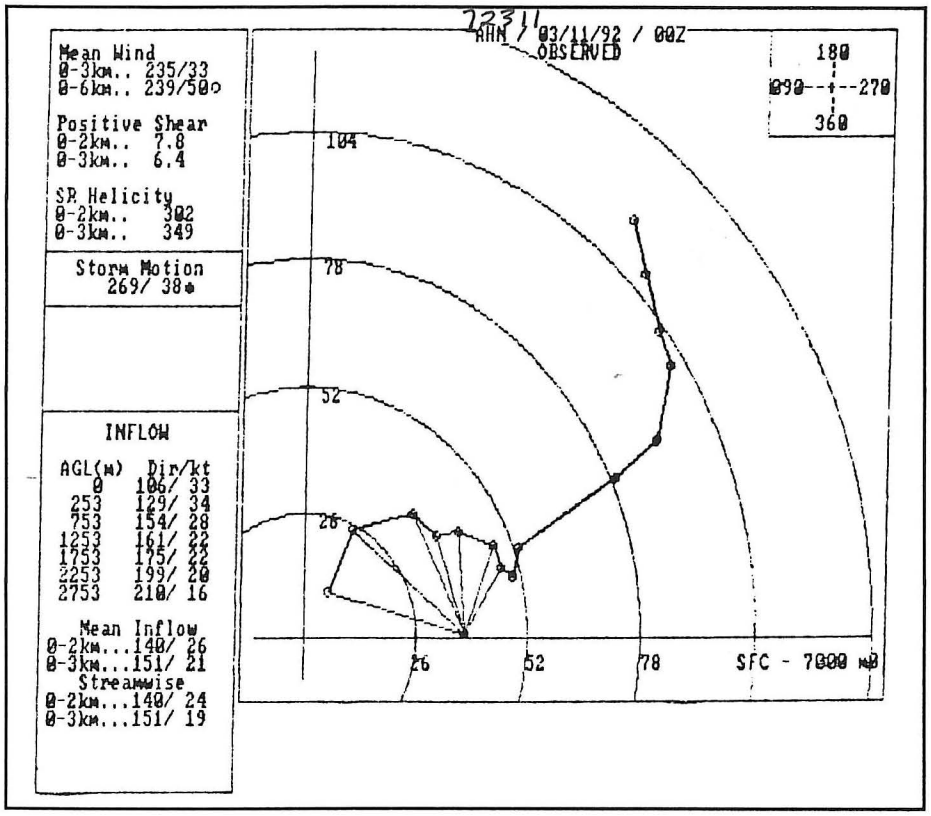

Fig. 10. AHN hodograph for 0000 UTC 11 March.

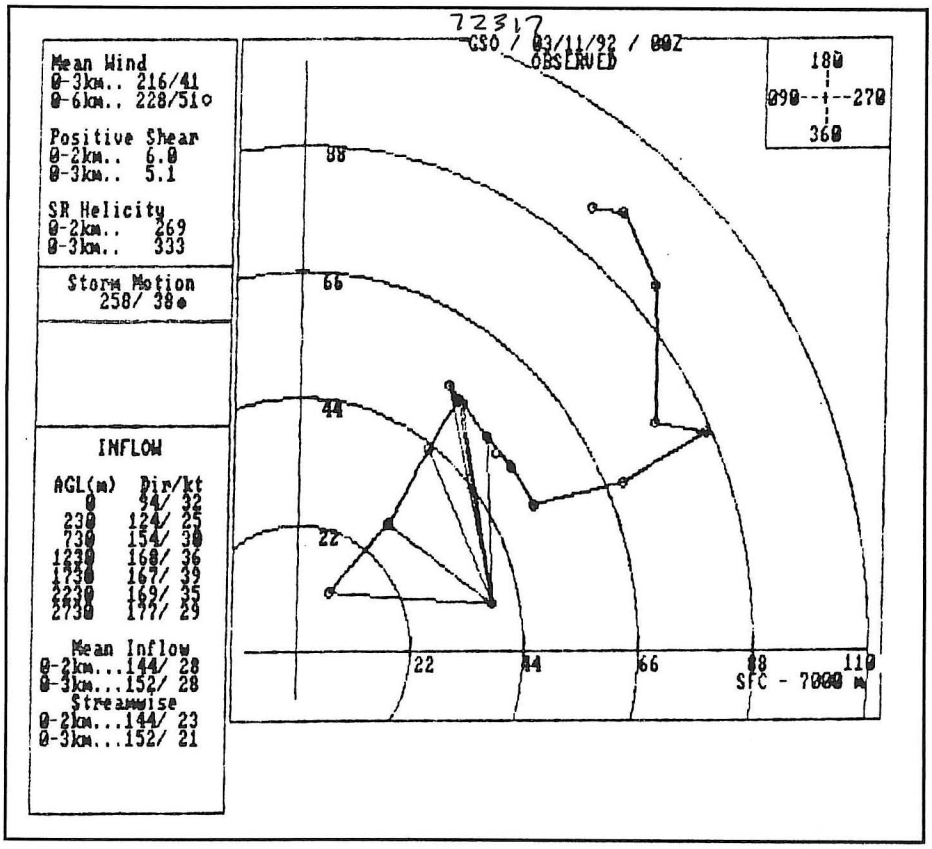

Fig. 11. GSO hodograph for 0000 UTC 11 March.

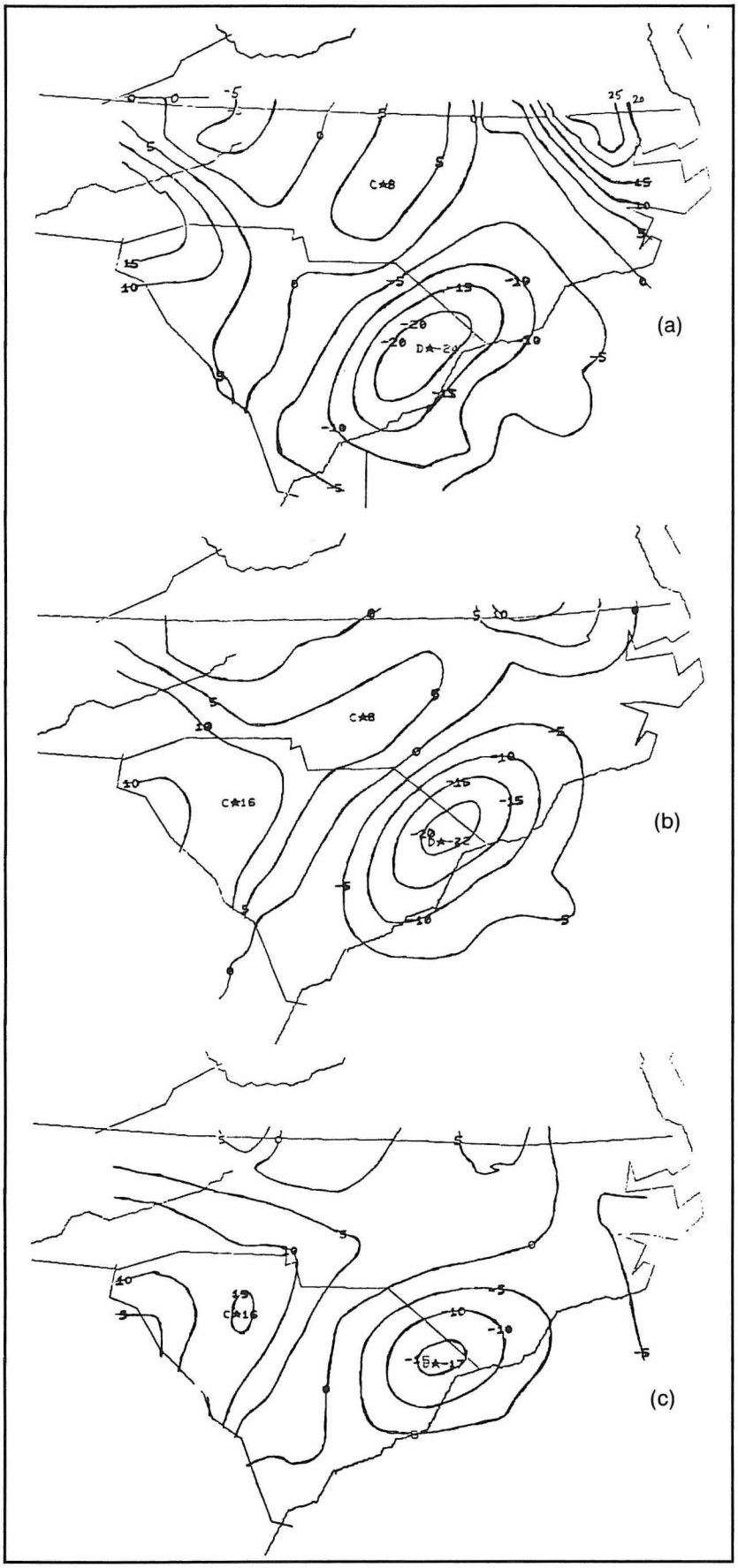

Fig. 12. Surface moisture flux convergence (g kg^{-1} hr^{-1} × 10) for (a) 0100 UTC 11 March, (b) 0200 UTC and (c) 0300 UTC.

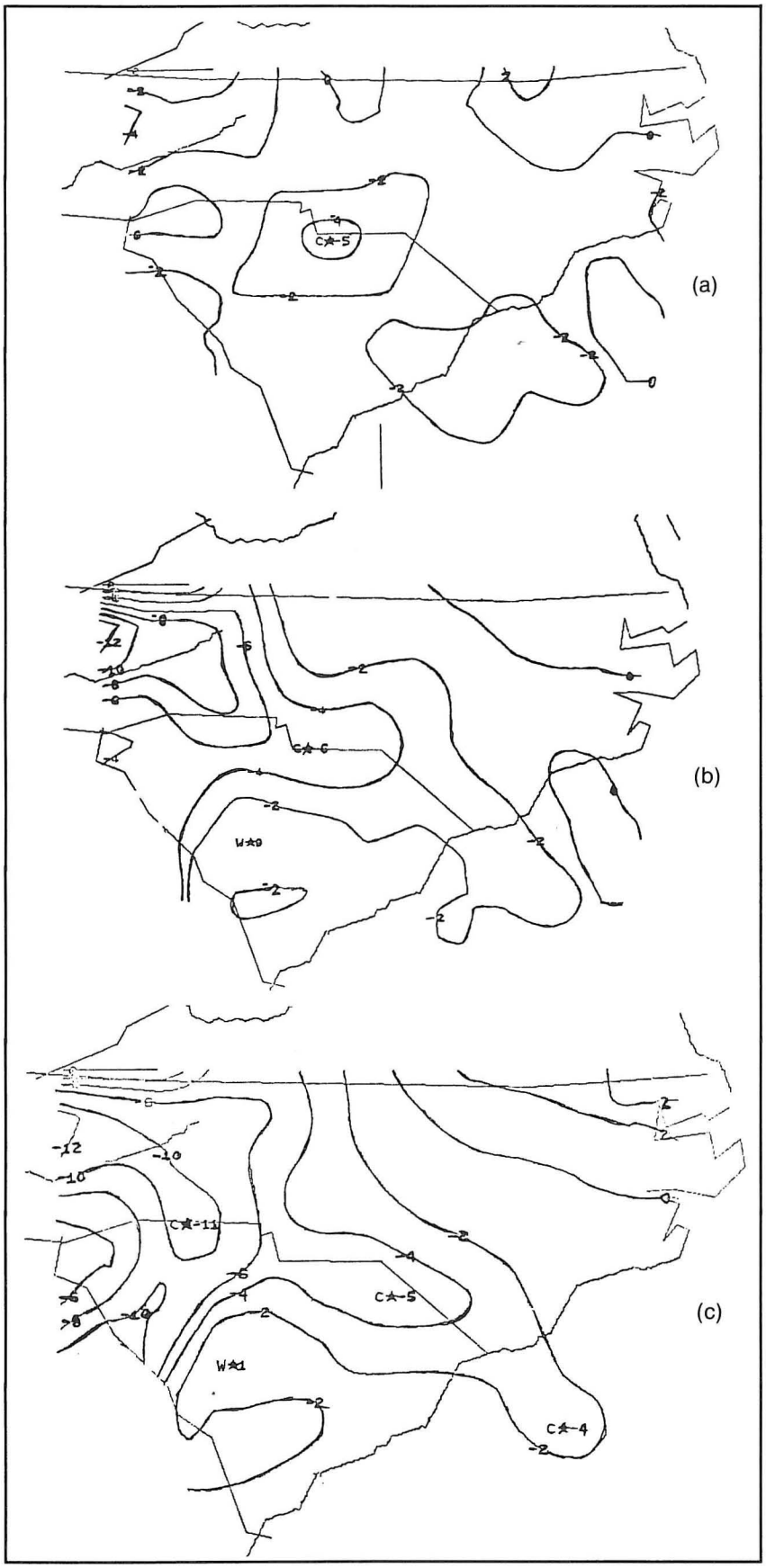

Fig. 13. Surface potential temperature (theta) advection (°F hr^{-1} for (a) 0100 UTC 11 March, (b) 0200 UTC and (c) 0300 UTC.

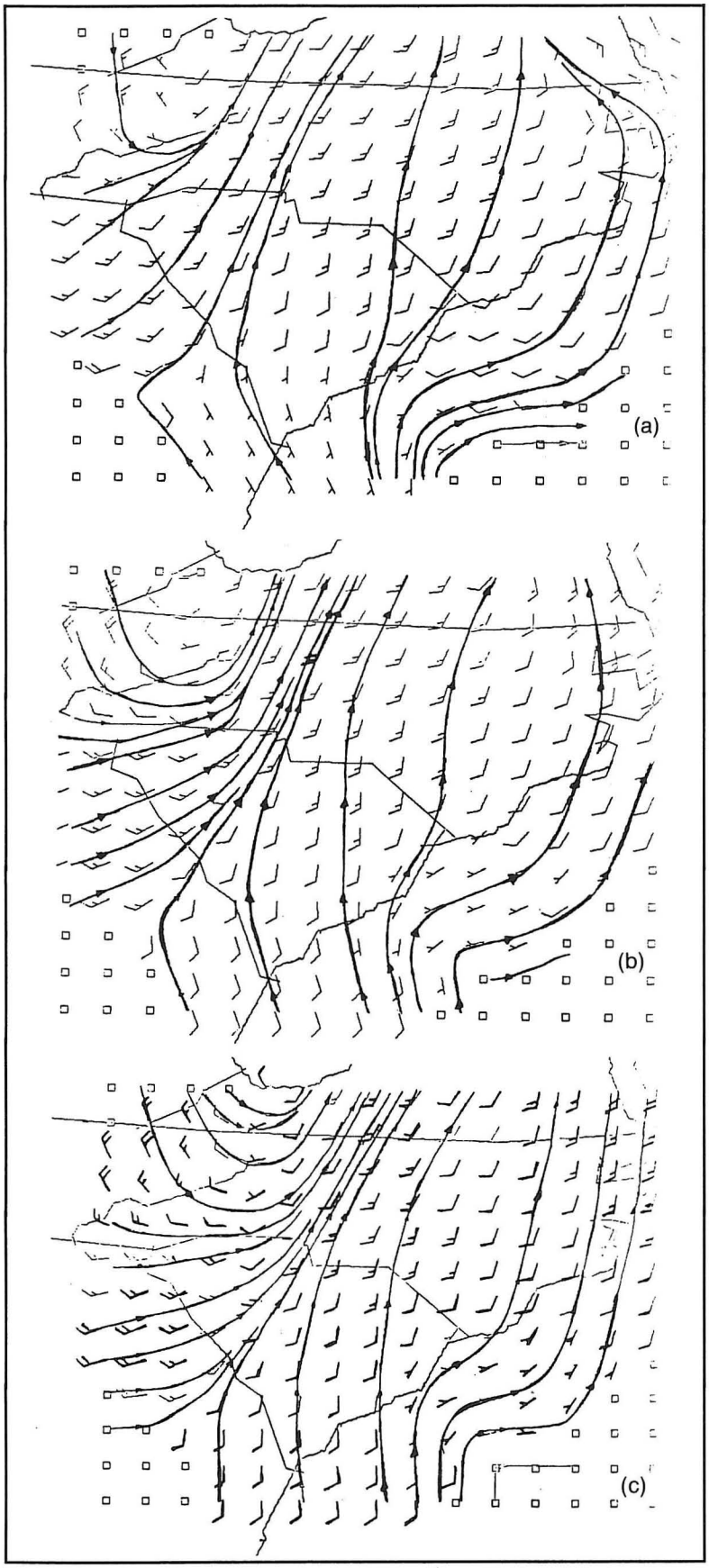

Fig. 14. Surface streamline analysis and wind plot for (a) 0100 UTC 11 March, (b) 0200 UTC and (c) 0300 UTC.

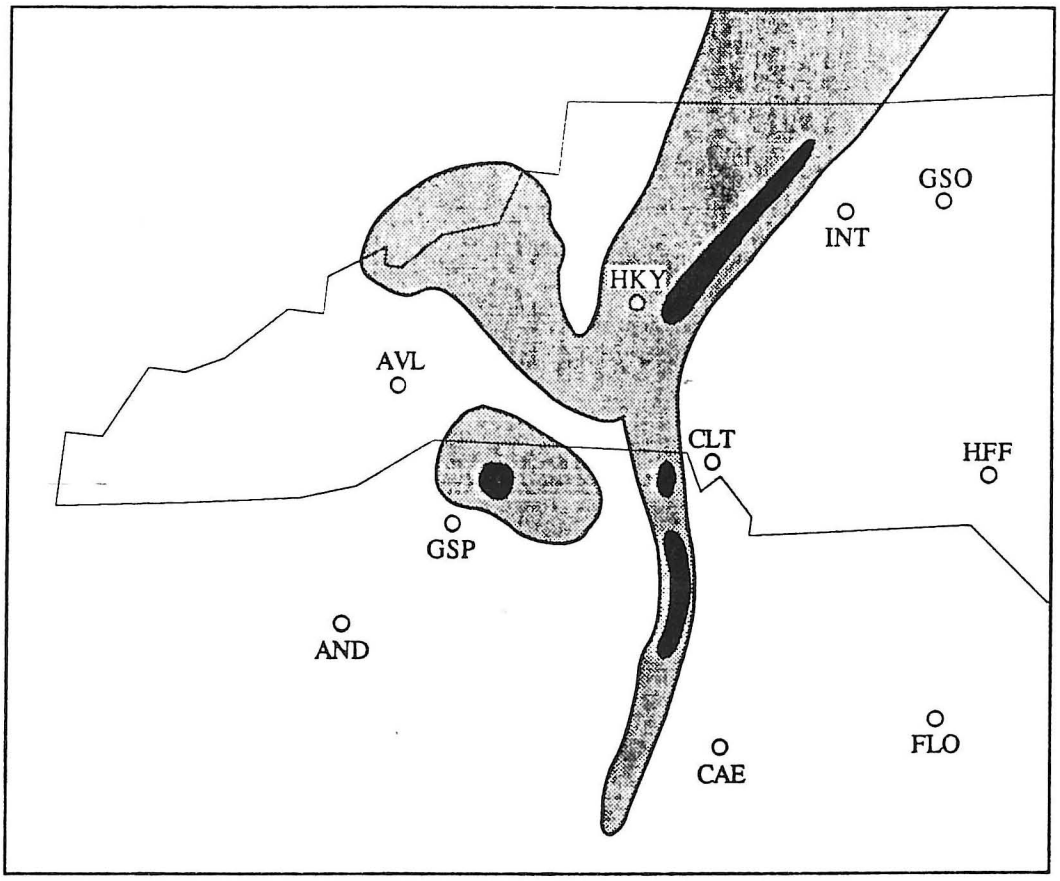

Fig. 15. Reflectivity as depicted by the radar at CLT at 0248 UTC. Elevation angle is 0.5°. Contours are DVIP levels 1 and 3.

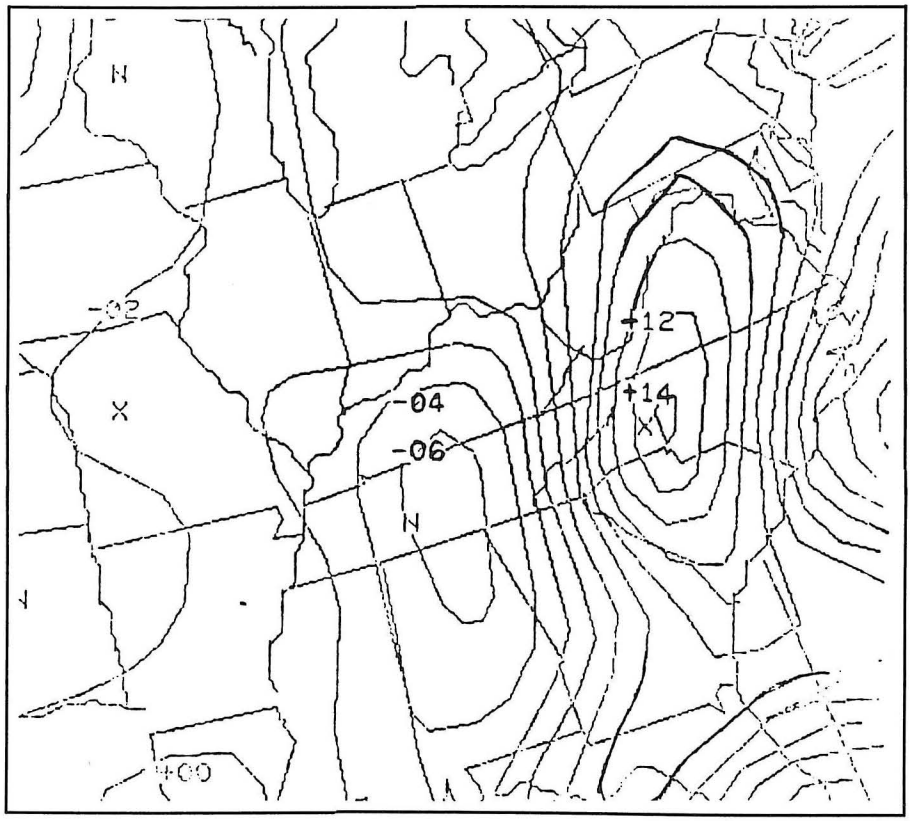

Fig. 16. Surface geostrophic vorticity ($\times 10^{-5}$ s^{-1}) analysis for 0300 UTC 11 March.

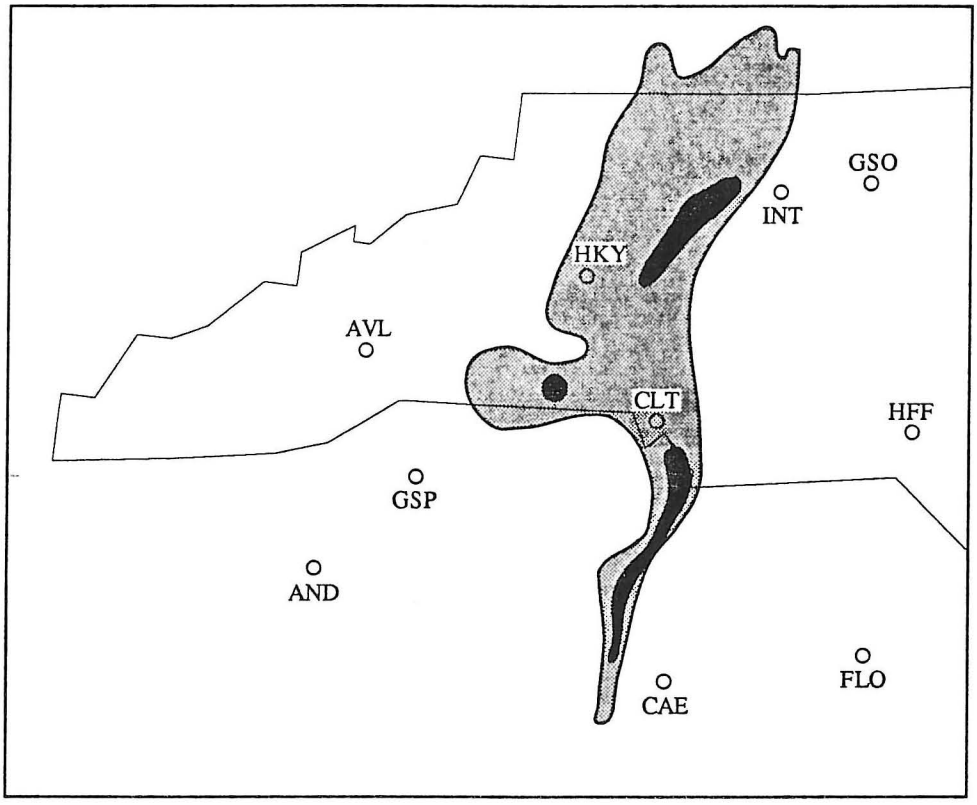

Fig. 17. Same as Fig. 15 except for 0301 UTC.

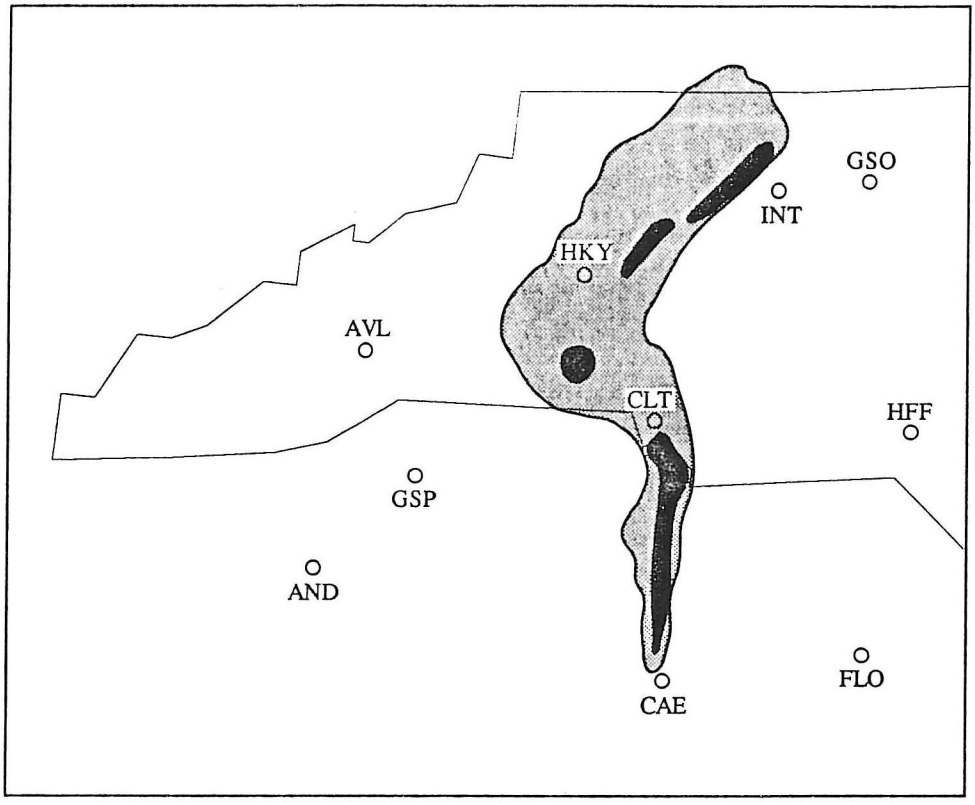

Fig. 18. Same as Fig. 15 except for 0314 UTC.